

The role of two-stage phase formation for the solid-state runaway reaction in Al/Ni reactive multilayers

Cite as: Appl. Phys. Lett. **117**, 011902 (2020); <https://doi.org/10.1063/5.0011338>

Submitted: 21 April 2020 . Accepted: 24 June 2020 . Published Online: 08 July 2020

T. Neuhauser , G. Tinti, H. Leiste , N. Casati , S. Ulrich, M. Stüber, and K. Woll 



View Online



Export Citation



CrossMark

ARTICLES YOU MAY BE INTERESTED IN

[Micrometer scale InGaN green light emitting diodes with ultra-stable operation](#)

Applied Physics Letters **117**, 011104 (2020); <https://doi.org/10.1063/5.0005436>

[Two-dimensional mechanical metamaterials with bending-induced expansion behavior](#)

Applied Physics Letters **117**, 011904 (2020); <https://doi.org/10.1063/5.0011876>

[Multilevel reversible laser-induced phase transitions in GeTe thin films](#)

Applied Physics Letters **117**, 011901 (2020); <https://doi.org/10.1063/5.0014375>



Instruments for Advanced Science

Contact Hiden Analytical for further details:

W www.HidenAnalytical.com

E info@hiden.co.uk

[CLICK TO VIEW](#) our product catalogue



Gas Analysis

- dynamic measurement of reaction gas streams
- catalysis and thermal analysis
- molecular beam studies
- dissolved species probes
- fermentation, environmental and ecological studies



Surface Science

- UHV/TPD
- SIMS
- end point detection in ion beam etch
- elemental imaging - surface mapping



Plasma Diagnostics

- plasma source characterization
- etch and deposition process reaction kinetic studies
- analysis of neutral and radical species



Vacuum Analysis

- partial pressure measurement and control of process gases
- reactive sputter process control
- vacuum diagnostics
- vacuum coating process monitoring

The role of two-stage phase formation for the solid-state runaway reaction in Al/Ni reactive multilayers

Cite as: Appl. Phys. Lett. **117**, 011902 (2020); doi: [10.1063/5.0011338](https://doi.org/10.1063/5.0011338)

Submitted: 21 April 2020 · Accepted: 24 June 2020 ·

Published Online: 8 July 2020



View Online



Export Citation



CrossMark

T. Neuhauser,¹  C. Tinti,² H. Leiste,³  N. Casati,²  S. Ulrich,³ M. Stüber,³ and K. Woll^{1,a)} 

AFFILIATIONS

¹Institute for Applied Materials (IAM-WBM), Karlsruhe Institute of Technology (KIT), 76344 Eggenstein-Leopoldshafen, Germany

²Paul Scherrer Institute, Swiss Light Source, 5232 Villigen/PSI, Switzerland

³Institute for Applied Materials (IAM-AWP), Karlsruhe Institute of Technology (KIT), 76344 Eggenstein-Leopoldshafen, Germany

^{a)} Author to whom correspondence should be addressed: karsten.woll@kit.edu

ABSTRACT

While extensively studied for heating rates below 1.7 K/s and above 1000 K/s, the solid-state phase transformations in Al/Ni reactive multilayers have not been examined at intermediate heating rates between 100 K/s and 1000 K/s. Combined nanocalorimetry and time-resolved synchrotron x-ray diffraction studies are utilized to address this range of heating rates for multilayers with an overall composition of 10 at. % Ni and a bilayer thickness of 220 nm. It was found that a two-stage phase formation of Al₃Ni proceeds up to a heating rate of 1000 K/s. The two growth stages occur in the solid-state and are kinetically separated. The activation energy of the first growth stage is determined to be 137 kJ/mol, which agrees well with the literature data at low heating rates. At 1000 K/s, a transition to a runaway reaction is observed. Unusual for metallic multilayers, the reaction proceeds completely in the solid-state which is also known as “solid flame.” Using nanocalorimetry, a critical input power density for ignition of 5.8×10^4 W/cm³ was determined. The rapid succession of the two Al₃Ni formation stages was identified as the underlying mechanism for the self-sustaining reaction.

© 2020 Author(s). All article content, except where otherwise noted, is licensed under a Creative Commons Attribution (CC BY) license (<http://creativecommons.org/licenses/by/4.0/>). <https://doi.org/10.1063/5.0011338>

Solid-state reactions in metallic nanopowders and multilayers have been studied for many years.^{1,2} One prominent example is the metal/Al reaction.^{3,4} The understanding is crucial in various fields such as microelectronics,⁵ the fabrication of micro- and nano-composites,⁶ or nanostructured reactive materials.⁷ Typical applications, like rapid soldering^{8,9} and the synthesis of high-temperature materials,¹⁰ exploit the exothermic reactions at the interfaces, including interdiffusion and phase transformation.¹¹ Fundamentally, nanoscale multilayers are used to explore solid-state reactions employing methods such as differential scanning calorimetry (DSC), transmission electron microscopy,^{12,13} or x-ray diffraction (XRD).¹⁴ The initial state with steep concentration gradients at the metal/Al interfaces is metastable.¹⁵ Numerous studies on binary Al-based systems observed phase selection where one particular phase, mostly the most Al-rich one, forms first,^{3,16,17} suggesting nucleation barrier minimization as the rate-limiting process.¹⁵ The Al/Ni system is one of the most intensively studied systems.^{18–23} During slow heating with maximal 1.7 K/s, Al₉Ni₂^{4,11,20,24} or Al₃Ni^{21,25–27} appears first depending on fabrication,

overall stoichiometry, and bilayer thickness (Λ). The formation of Al₃Ni often occurs in two stages.^{1,4,21,25,28} Nucleation and growth along the interfaces precedes the growth perpendicular to the interfaces. Experiments using DSC reveal two characteristic exothermic peaks demonstrating the kinetic separation of the two stages pointing to the relevance of nucleation barriers.²⁵ Although only little investigated, Al₃Ni is also the first phase to form under high heating rates up to 10⁵ K/s.^{13,29}

The solid-state reaction may turn into a runaway reaction under sufficiently high heating rates. The reaction power related to exothermic heat release by interdiffusion and phase formation increases with the heating rate and starts to overcompensate the heat losses to the surrounding once a critical heating rate is achieved. The reaction becomes self-sustaining where no external heating is required for reaction progress.³⁰ During self-sustaining reactions, temperatures are usually above the melting temperature of Al and the transformation proceed at a liquid-solid interface.³¹ Contrasting the solid-state reactions, the reactions during the runaway are not fully elucidated.^{31–33}

Solid-state reactions, including interdiffusion and phase nucleation, potentially initiate the runaway reaction, which accelerates once a liquid Al/solid Ni interface forms.³¹ Only recently, we were able to elucidate the nature of the evolving phases.¹⁴ For ignition with 5000 K/s, the heat of mixing released by interdiffusion is sufficient to initiate the reaction. Hence, the solid-state phase selection observed during slow heating does not seem to be critical for the runaway reaction ignited with heating rates > 5000 K/s.

Interestingly, it was recently experimentally verified^{34–36} that runaway reactions may also proceed in the solid state, sometimes called as ideal solid flame. The melting points of the reactants and products have to be higher than the adiabatic reaction temperature. Hence, it is ambiguous whether systems with a low-melting metal, such as Al/Ni, are able to show a solid-state runaway. In fact, few studies were able to infer reactions in the solid flame regime for Al/Ni powders.^{36,37}

While extensively studied at low and high heating rates, there is a gap in understanding of the reactions under intermediate heating rates between 1.7 K/s and 1000 K/s. However, the transition from solid-state to runaway reactions occurs in this unexplored heating rate regime. Questions regarding the transformation behavior in this heating rate regime and its role for the transition from solid-state to runaway reactions are so far unanswered impeding the development of a mechanism based knowledge. The current study provides answers to these questions. We use Al/Ni multilayers as model materials to develop a mechanism for the transition from solid-state to runaway reactions when heating rates are increased. It is found that the two-stage formation of Al₃Ni proceeds at heating rates above 100 K/s as well as under runaway conditions. For 1000 K/s, the solid-state reaction turns into a “solid flame”^{34,35} which is reported for the first time for nanoscale Al/Ni multilayers.

Al/Ni multilayers with a thickness of 2 μm were DC-magnetron sputtered from pure Al ($>99.995\%$) and Ni ($>99.95\%$) targets. The nominal overall composition and the bilayer thickness was 10 at. % Ni and 220 nm, respectively. The sputter rates were 21 nm/min for Al and 39 nm/min for Ni. The chamber base pressure was $< 2 \times 10^{-4}$ Pa, and high purity argon ($>99.999\%$) was used as sputter gas. The multilayers were deposited on nanocalorimeter sensors to heat and thermally analyze the reactions. Nanocalorimetry is a chip-based calorimetry technique, which allows for the quantification of heat release from the interface reactions of thin films under heating rates $< 10^6$ K/s.^{38–40} Reaction power and heat losses are measured during heating enabling us to quantify ignition. For *in situ* structural analysis, nanocalorimetry was combined with time-resolved synchrotron x-ray diffraction at the X04SA powder diffraction beamline of the Swiss Light Source (SLS) of the Paul Scherrer Institute (PSI, Villigen, Switzerland).⁴¹ A beam energy of 12.6 keV (0.984 Å) and a spot size of $500 \times 500 \mu\text{m}^2$ was used in transmission. The diffracted signal was captured with a PSI developed 2D single photon counting area detector (Eiger 500k)^{42,43} with an acquisition rate between 400 and 5000 Hz. Details can be found in our previous study.¹⁴

Al/Ni multilayers were heated with 100 K/s, 500 K/s, and 1000 K/s, as shown in Fig. 1(a). Two well separated exotherms for the 100- and 500-K/s-experiments indicate phase transformations. In the case of 100 K/s, the peak onset is at 343 °C, while the second peak starts at ~ 407 °C. These peaks are substantially more pronounced for heating with 500 K/s due to the increased reaction power \dot{Q}_{ret} compared to 100 K/s. The peak onset of the first and second peak

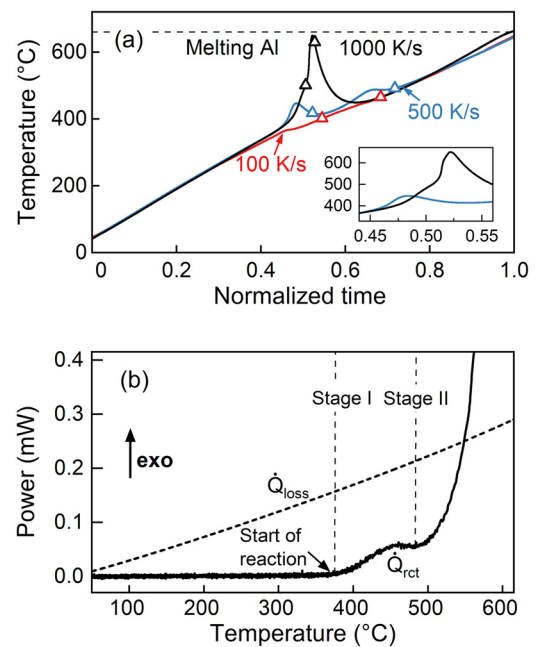


FIG. 1. (a) Temperature vs time measured by nanocalorimetry for the indicated heating rates. The inset reveals a shoulder in the signal which occurs when the specimen is heated with 1000 K/s. The triangles indicate temperatures, where x-ray diffractograms were taken as shown in Fig. 3(a). (b) The power contributions of the 1000-K/s-experiment in (a). The reaction power \dot{Q}_{ret} (solid line) starts to overcompensate for the heat losses \dot{Q}_{loss} (dashed line) for temperature > 550 °C indicating a runaway reaction.

shifts with heating rate by +38 °C and +24 °C, respectively, which is typical for nucleation and growth processes. For the 1000-K/s-experiment, the two peaks merge to one pronounced temperature peak with a low-temperature shoulder between 400 °C and 500 °C [compare inset of Fig. 1(a)]. The corresponding \dot{Q}_{ret} signal shown in Fig. 1(b) exhibits the separation of the two exothermic peaks, enabling us to denote two stages. In addition, we observe a temperature increase of 255 °C within 40 ms, suggesting a transition from a solid-state to a runaway reaction.

To prove the presence of a runaway reaction for 1000 K/s, we consider that a runaway reaction is self-sustaining and deduce the mandatory criterion $\dot{Q}_{\text{ret}} > \dot{Q}_{\text{loss}}$, where \dot{Q}_{loss} denote the heat losses. \dot{Q}_{ret} and \dot{Q}_{loss} are plotted in Fig. 1(b). $\dot{Q}_{\text{ret}} > \dot{Q}_{\text{loss}}$ is fulfilled for temperatures > 550 °C confirming a self-sustaining reaction. The critical input power density for ignition is 5.8×10^4 W/cm³ which is in reasonable agreement with literature values for Al/Ni multilayers.^{31,32}

Noticeably, the runaway reaction is a solid-state reaction since the maximal temperature of 650 °C is below the melting temperatures of all reactants and products (Al = 660 °C, Al₃Ni = 845 °C, and Ni = 1455 °C). To the authors' knowledge, this is the first time that a solid-state runaway reaction is observed for metallic multilayers. This contrasts observations, where the runaway is ignited in the solid state and proceeds by the presence of a liquid phase at rates ≥ 5000 K/s.^{14,31,44,45} The presence of a liquid phase is usually considered as a necessary condition for runaway reactions because the intermixing rates are significantly enhanced.⁴⁶

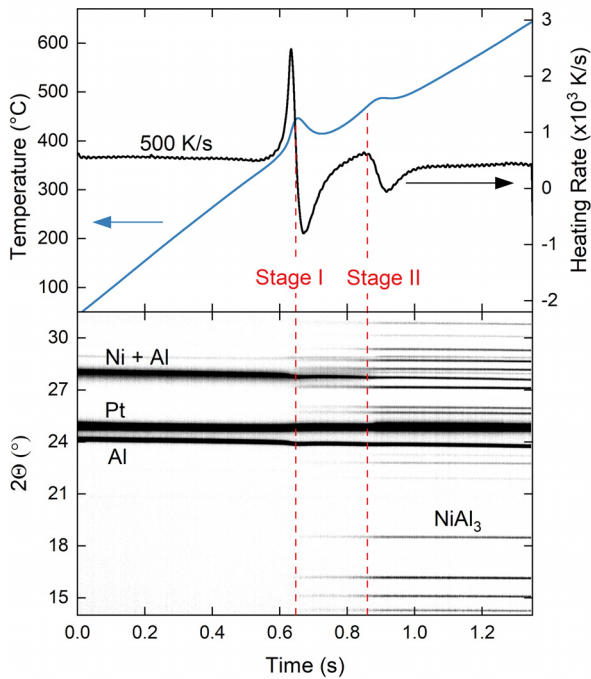


FIG. 2. Top: temperature (blue) and heating rate (black) for Al/Ni multilayers heated with 500 K/s. Bottom: corresponding *in situ* x-ray diffraction (XRD) signal. The individual stages are marked in red. The Pt peak ($2\theta_{\text{Pt}(111)} = 24.84^\circ$) is generated by the nanocalorimetry sensor.

Next, we analyze the underlying phase transformation. Figure 2 shows variations in temperature and heating rate for 500 K/s. The time-resolved x-ray diffraction data are plotted in the lower part of Fig. 2 and relate the temperature evolution to the phase transformations of the sample. Based on the ICSD database,⁴⁷ a peak of Al ($2\theta_{\text{Al}(111)} = 24.11^\circ$) and an overlapping Al + Ni peak ($2\theta_{\text{Al}(111),\text{Ni}(200)} = 27.95^\circ$) were identified for the course of the reaction corroborating the solid-state transformations [see Fig. 3(a)]. During the first exothermic peak at 385 °C, diffraction peaks of the Al₃Ni phase start to appear. The corresponding peak intensity qualitatively grows in two stages, denoted as stage I and stage II, with a substantial increase during the second exothermic peak in the temperature signal.

Simultaneously, the intensity of the superimposed Ni + Al peak decreases, which we attribute to the consumption of Ni and Al with reaction progress. Hence, whereas nanocalorimetry reveals two kinetically separated exothermic solid-state reactions, the time-resolved diffraction experiment identifies the growth of only one compound, namely, Al₃Ni.

To visualize the exclusive growth of Al₃Ni, Fig. 3(a) plots the *in situ* recorded diffractograms after the first and second exothermic peak in the nanocalorimetry experiment [compare Fig. 1(a)]. In addition to the elemental peaks, only XRD peaks of the Al₃Ni phase can be identified. Independent of the heating rate, Al₃Ni peaks are present after the first exothermic peak and grow in intensity after the second one. The Al peak at 23.86° is permanently present for all heating rates. Since Al is the reactant with the lowest melting point involved, we conclude that all reactions take place in the solid-state of the sample. This

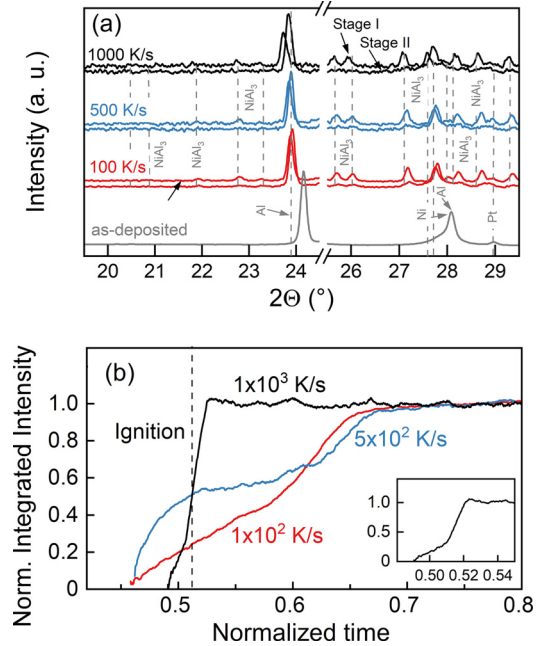


FIG. 3. (a) Individual diffractograms recorded during the time-resolved experiments for 100 K/s (red), 500 K/s (blue), and 1000 K/s (black). The temperatures, where the diffractograms were recorded, are marked with triangles in Fig. 1(a). A representative diffractogram of an as-deposited sample is shown in gray. (b) Normalized integrated intensity $I_{\text{Al}_3\text{Ni}}$ for the Al₃Ni peaks vs normalized heating time. The inset shows $I_{\text{Al}_3\text{Ni}}$ of the solid-state runaway.

corroborates that a runaway reaction like observed at 1000 K/s is not limited to the liquid state, but it can also occur in the solid-state of Ni/Al. For more detailed insights into the growth behavior of Al₃Ni, we calculated the temporal evolution of the integrated peak intensity as a sum of the Al₃Ni-peaks in the range of 13.78°–18.51° and 21.93°, 22.81°, 25.73°, 26.05°, and 30.19°. Figure 3(b) plots the normalized integrated intensity $I_{\text{Al}_3\text{Ni}}$ as a function of the normalized time. For the 100-K/s- and 1000-K/s-experiments, Fig. 3(b) reveals a change in the $I_{\text{Al}_3\text{Ni}}$ increase indicating a transition in the phase growth rate at 0.5 and 0.32, respectively. For the 500-K/s-experiment, a plateau of $I_{\text{Al}_3\text{Ni}}$ at 0.6 is observed. Hence, the $I_{\text{Al}_3\text{Ni}}$ evolution suggests the effects of the heating rate on the Al₃Ni growth kinetics. As shown in Fig. 1(a), the heating rate is almost constant for the 100-K/s-experiment with no additional temperature rise due to the solid-state reaction. This results in a continuous growth of Al₃Ni in stage I. The transition from an interfacial growth at the Al/Ni interface (stage I) to a growth perpendicular to the interface (stage II) is indicated by a change in the slope at 0.5 shown in Fig. 3(b). The growth behavior changes when the heating rate is increased to 500 K/s. The Al₃Ni formation between $0 < I_{\text{Al}_3\text{Ni}} < 0.4$ results in an enhanced reaction power at 500 K/s, causing the pronounced temperature increase of 38 °C [see Fig. 1(a)]. Assuming an Arrhenius dependency of the phase growth kinetics, the temperature increase accelerates the Al₃Ni growth along the interfaces which is quickly saturated and creates the plateau in $I_{\text{Al}_3\text{Ni}}$. Before stage II is initiated at 450 °C, there is only minor phase formation. Based on the transition in the $I_{\text{Al}_3\text{Ni}}$ evolution, the results for 100 K/s and 500 K/s allow us to estimate that stage I is completed for 0.5

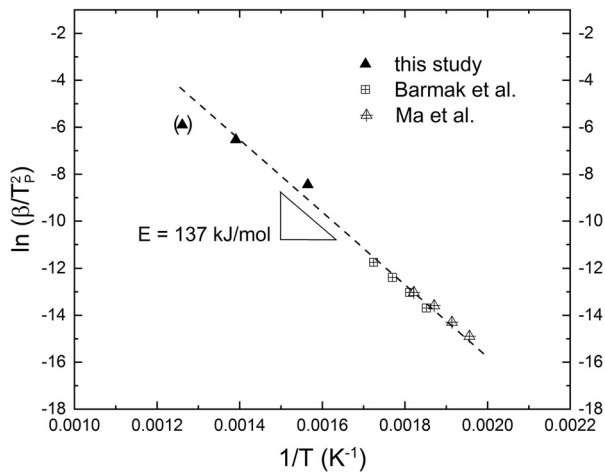


FIG. 4. Kissinger plot of the Al_3Ni nucleation and growth stage. The measurements from the current study (full triangles) are compared to that determined by Barmak *et al.*⁴ (open squares) and Ma *et al.*²⁵ (open triangles).

$< I_{\text{Al}_3\text{Ni}} < 0.6$. Under 1000 K/s, we observe the transition already at 0.32, suggesting the incomplete transition of stage I. The early stages of nucleation and growth release enough reaction power to increase the temperature above 550 °C and to initiate stage II before stage I is completed. We note that ignition (compare dashed line) occurs when 0.5 phase formation is observed, which points out that the two-stage mechanism can contribute to a runaway reaction in the solid-state. This transition from a solid-state to a solid-state runaway reaction at elevated heating rates expands the knowledge from low heating rates below 1.7 K/s.^{4,21,25,28,48,49}

In order to prove whether the observed two-stage growth of Al_3Ni is governed by interfacial nucleation and growth (stage I) followed by growth perpendicular to the interfaces (stage II),⁴⁸ a kinetic analysis of stage I was performed. As the heating rate β is increased, the corresponding shifts in the peak temperature T_p in Fig. 1(a) are used to create a Kissinger plot ($\ln(\frac{\beta}{T_p^2})$ vs T_p^{-1}), as shown Fig. 4. The activation energy is deduced from the slope of the Kissinger plot. Complementary published data on Al_3Ni nucleation and growth along the interfaces determine an activation energy of ≈ 137 kJ/mol for heating rates < 1.7 K/s (indicated by the dashed line).^{4,25} The data of the present study are in reasonable agreement with the kinetic analysis in the literature. Hence, we conclude that Al_3Ni nucleation and its growth along the interfaces presumably dominates in stage I up to at least 500 K/s. Since the completion as well as a kinetic separation of stage I is not observed for the solid-state reaction under 1000 K/s, we included the data for completeness.

In summary, we combined nanocalorimetry with time-resolved synchrotron x-ray diffraction to explore phase transformations in Al/Ni multilayers for heating rates of 100 K/s, 500 K/s and 1000 K/s. The results are summarized as follows:

- For all considered heating rates, Al_3Ni is the only phase formed. The thermal and structural analysis reveals that phase formation occurs in two kinetically separated stages in the solid state up to a heating rate of 1000 K/s. The kinetic analysis of the phase

formation under 100 K/s and the 500 K/s suggests that the two-stage mechanism comprises nucleation and growth along the interface, succeeded by phase growth perpendicular to the interfaces. This is in good agreement with the literature data observed for 1.7 K/s.

- For 1000 K/s, the kinetic separation in the nanocalorimetry data is less pronounced, suggesting that the rapid succession of both Al_3Ni formation stages leads to a runaway reaction. This runaway proceeds completely in the solid state and shows similarities to the solid flame phenomenon, which is observed for the first time in metallic multilayers.

K.W. and T.N. gratefully acknowledge the financial support of the German Research Foundation (DFG) within the Emmy-Noether-Program (Funding No. WO 2198/1-1). The research leading to these results has received funding from the European Union's Horizon 2020 research and innovation programme under Grant Agreement No. 730872, project CALIPSOplus.

DATA AVAILABILITY

The data that support the findings of this study are available from the corresponding author upon reasonable request.

REFERENCES

- ¹C. Michaelsen, K. Barmak, and T. P. Weihs, *J. Phys. D: Appl. Phys.* **30**, 3167 (1997).
- ²A. S. Mukasyan and C. E. Shuck, *Int. J. Self-Propagating High-Temp. Synth.* **26**, 145 (2017).
- ³E. G. Colgan, *Mater. Sci. Rep.* **5**, 1 (1990).
- ⁴K. Barmak, C. Michaelsen, and G. Lucadamo, *J. Mater. Res.* **12**, 133 (1997).
- ⁵J. Wang, E. Besnoin, A. Duckham, S. J. Spey, M. E. Reiss, O. M. Knio, M. Powers, M. Whitener, and T. P. Weihs, *Appl. Phys. Lett.* **83**, 3987 (2003).
- ⁶A. S. Edelstein, R. K. Everett, G. R. Richardson, S. B. Qadri, J. C. Foley, and J. H. Perepezko, *Mater. Sci. Eng., A* **195**, 13 (1995).
- ⁷D. P. Adams, *Thin Solid Films* **576**, 98 (2015).
- ⁸J. Wang, E. Besnoin, A. Duckham, S. J. Spey, M. E. Reiss, O. M. Knio, and T. P. Weihs, *J. Appl. Phys.* **95**, 248 (2004).
- ⁹C. Rossi, K. Zhang, D. Estève, P. Alphonse, P. Tailhades, and C. Vahlas, *J. Microelectromech. Syst.* **16**, 919 (2007).
- ¹⁰A. G. Merzhanov, *J. Mater. Chem.* **14**, 1779 (2004).
- ¹¹A. S. Edelstein, R. K. Everett, G. Y. Richardson, S. B. Qadri, E. I. Altman, J. C. Foley, and J. H. Perepezko, *J. Appl. Phys.* **76**, 7850 (1994).
- ¹²M. D. Grapes, T. Lagrange, L. H. Friedman, B. W. Reed, G. H. Campbell, T. P. Weihs, and D. A. Lavan, *Rev. Sci. Instrum.* **85**, 084902 (2014).
- ¹³M. D. Grapes, T. P. Weihs, M. K. Santala, H. Campbell, and D. A. Lavan, *Thermochim. Acta* **658**, 72 (2017).
- ¹⁴T. Neuhauser, G. Tinti, H. Leiste, N. Casati, M. Stüber, and K. Woll, *Acta Mater.* **195**, 579 (2020).
- ¹⁵C. Michaelsen, G. Lucadamo, and K. Barmak, *J. Appl. Phys.* **80**, 6689 (1996).
- ¹⁶E. G. Colgan and J. W. Mayer, *J. Mater. Res.* **4**, 815 (1989).
- ¹⁷R. Pretorius, R. de Reus, A. M. Vredenberg, and F. W. Saris, *Mater. Lett.* **9**, 494 (1990).
- ¹⁸E. Ma, C. V. Thompson, L. A. Clevenger, and K. N. Tu, *Appl. Phys. Lett.* **57**, 1262 (1990).
- ¹⁹A. J. Gavens, D. Van Heerden, A. B. Mann, M. E. Reiss, and T. P. Weihs, *J. Appl. Phys.* **87**, 1255 (2000).
- ²⁰K. J. Blobaum, D. Van Heerden, A. J. Gavens, and T. P. Weihs, *Acta Mater.* **51**, 3871 (2003).
- ²¹A. Ustinov, L. Olikhovska, T. Melnichenko, and A. Shyshkin, *Surf. Coat. Technol.* **202**, 3832 (2008).
- ²²R. Knepper, M. R. Snyder, G. Fritz, K. Fisher, O. M. Knio, and T. P. Weihs, *J. Appl. Phys.* **105**, 083504 (2009).

- ²³M. D. Grapes and T. P. Weihs, *Combust. Flame* **172**, 105 (2016).
- ²⁴A. I. Ustinov and S. A. Demchenkov, *Intermetallics* **84**, 82 (2017).
- ²⁵E. Ma, C. V. Thompson, and L. A. Clevenger, *J. Appl. Phys.* **69**, 2211 (1991).
- ²⁶T. Jeske, M. Seibt, and G. Schmitz, *Mater. Sci. Eng., A* **353**, 105 (2003).
- ²⁷M. Swain, S. Singh, S. Basu, and M. Gupta, *J. Alloys Compd.* **576**, 257 (2013).
- ²⁸E. Ma, M. Nicolet, and M. Nathan, *J. Appl. Phys.* **65**, 2703 (1989).
- ²⁹M. D. Grapes, T. Lagrange, K. Woll, B. W. Reed, G. H. Campbell, D. A. Lavan, and T. P. Weihs, *APL Mater.* **2**, 116102 (2014).
- ³⁰I. Glassman, A. R. Yetter, and G. N. Glumac, *Combustion*, 5th ed. (Elsevier, 2015).
- ³¹G. M. Fritz, J. A. Grzyb, O. M. Knio, M. D. Grapes, and T. P. Weihs, *J. Appl. Phys.* **118**, 135101 (2015).
- ³²G. M. Fritz, S. J. Spey, M. D. Grapes, and T. P. Weihs, *J. Appl. Phys.* **113**, 014901 (2013).
- ³³K. V. Manukyan, J. M. Pauls, C. E. Shuck, S. Rouvimov, A. S. Mukasyan, K. Nazaretyan, H. Chatilyan, and S. Kharatyan, *J. Phys. Chem. C* **122**, 27082–27092 (2018).
- ³⁴A. S. Mukasyan, C. E. Shuck, J. M. Pauls, K. V. Manukyan, D. O. Moskovskikh, and A. S. Rogachev, *Adv. Eng. Mater.* **20**, 1701065 (2018).
- ³⁵A. G. Merzhanov, *Combust. Sci. Technol.* **98**, 307 (1994).
- ³⁶C. E. Shuck, K. V. Manukyan, S. Rouvimov, A. S. Rogachev, and A. S. Mukasyan, *Combust. Flame* **163**, 487 (2016).
- ³⁷A. S. Mukasyan, J. D. E. White, D. Y. Kovalev, N. A. Kochetov, V. I. Ponomarev, and S. F. Son, *Physica B* **405**, 778 (2010).
- ³⁸C. Schick, *Fast Scanning Calorimetry* (Springer International Publishing, 2016).
- ³⁹F. Yi and D. A. LaVan, *Appl. Phys. Rev.* **6**, 031302 (2019).
- ⁴⁰Y. Gao, B. Zhao, J. J. Vlassak, and C. Schick, *Prog. Mater. Sci.* **104**, 53 (2019).
- ⁴¹P. R. Willmott, D. Meister, S. J. Leake, M. Lange, and A. Bergamaschi, *J. Synchrotron Radiat.* **20**, 667 (2013).
- ⁴²R. Dinapoli, A. Bergamaschi, D. Greiffenberg, B. Henrich, R. Horisberger, I. Johnson, A. Mozzanica, V. Radicci, B. Schmitt, X. Shi, and G. Tinti, *Nucl. Instrum. Methods Phys. Res., Sect. A* **731**, 68 (2013).
- ⁴³I. Johnson, A. Bergamaschi, H. Billich, S. Cartier, R. Dinapoli, D. Greiffenberg, M. Guizar-Sicairos, B. Henrich, J. Jungmann, D. Mezza, A. Mozzanica, B. Schmitt, X. Shi, and G. Tinti, *J. Instrum.* **9**, C05032 (2014).
- ⁴⁴J. C. Trenkle, L. J. Koerner, M. W. Tate, N. Walker, S. M. Gruner, T. P. Weihs, and T. C. Hufnagel, *J. Appl. Phys.* **107**, 113511 (2010).
- ⁴⁵K. Fadenberger, I. E. Gunduz, C. Tsotsos, M. Kokonou, S. Gravani, S. Brandstetter, A. Bergamaschi, B. Schmitt, P. H. Mayrhofer, C. C. Doumanidis, and C. Rebholz, *Appl. Phys. Lett.* **97**, 144101 (2010).
- ⁴⁶A. S. Rogachev, S. G. Vadchenko, and A. S. Mukasyan, *Appl. Phys. Lett.* **101**, 063119 (2012).
- ⁴⁷F. I. Z. Karlsruhe, *ICSD Inorganic Crystal Structure Database* (FIZ Karlsruhe, 2020).
- ⁴⁸K. R. Coffey, L. A. Clevenger, K. Barmak, D. A. Rudman, and C. V. Thompson, *Appl. Phys. Lett.* **55**, 852 (1989).
- ⁴⁹K. J. Blobaum, A. J. Wagner, J. M. Plitzko, D. Van Heerden, D. H. Fairbrother, and T. P. Weihs, *J. Appl. Phys.* **94**, 2923 (2003).